Journal of Biomolecular Structure & Dynamics, ISSN 0739-1102
Conversation 11, Issue #2 (2000) 0-940030-81-0
Proceedings of the Eleventh Conversation, University at Albany, SUNY, June 15-19, 1999

Nucleic Acid Structure Investigated by UV Resonance Raman Spectroscopy: Protonation Effects and A-Tract Structure

http://www.adeninepress.com/jbsd

Liliana Sokolov, Kristi Wojtuszewski, Eliana Tsukroff† and Ishita Mukerji*
Molecular Biology and Biochemistry Department and †Department of Chemistry, Molecular Biophysics Program, Wesleyan University, Middletown, CT 06459-0175

Abstract

UV resonance Raman (UVRR) spectroscopy has been used to investigate the three purine bases, adenine, guanine and inosine, as a function of pH. Excitation wavelengths of 260 and 210 nm were used to probe the in-plane ring stretching frequencies and the exocyclic functional groups, respectively. These studies are suggestive that tautomeric forms can be stabilized at low and high pH values and these forms can be identified using UVRR spectroscopy. At pH values ≤ 5.0, a band at 1693 cm^{-1} is observed in the UVRR spectra of dAMP, which is suggestive of the imino protonated tautomer. At pH values of 10.0 and above both dGMP and IMP show evidence for forming the enolate tautomer, by the loss in intensity of the C=O stretching mode at 1686 cm^{-1}. The protonated forms of dGMP and dAMP exhibit distinct Raman bands at approximately 1460 and 1561 cm^{-1} and we suggest that these protonated states can be identified using UVRR spectroscopy. Most distinctively, the $-NH_2$ scissors mode of dGMP and dAMP shifts up in frequency and increases in intensity as the pH is decreased. Interestingly, these features are also observed in a comparison of an A-tract containing dodecamer with a non A-tract dodecamer. In particular, a frequency upshift of the $-NH_2$ scissors mode and a mode at 1466 cm^{-1} is observed. Because of the resonance enhancement and the similarities to the protonated dAMP spectrum, these features are attributed to the dA residues in the A-tract. It is suggested that these spectral features may be characteristic of 'bent' DNA.

Introduction

Vibrational spectroscopy has been applied to numerous problems in the study of nucleic acid structure. Structural changes associated with base stacking, duplex melting, metal ion coordination and H-bonding are detected by intensity changes and frequency shifts. More recently, the technique of UV resonance Raman (UVRR) spectroscopy has been applied to the study of nucleic acid structure (1-6). This spectroscopic technique utilizes electronic transitions to enhance the Raman signal by at least 10^3, which leads not only to signal enhancement but also to nucleic acid residue and mode selectivity (7,8). For instance, shorter excitation wavelengths (~210 nm) enhance the C = O modes of guanosine and inosine which are not observed when longer excitation wavelengths are used (3,5,7).

However, in order to interpret the spectra of DNA and RNA obtained with this technique, the effects of H-bonding and protonation on the spectra of the individual nucleic acids should be well-characterized. Cytosine in the protonated state has been studied extensively using UVRR spectroscopy (2,9), but protonation and deprotonation effects of the other nucleic acid bases have not been studied systematically using this approach (10,11). Many of these studies have been conducted using Raman spectroscopy, but because of the differences in the enhancement patterns and the lower concentrations that can be used, we have revisited them using UVRR spectroscopy.

*Phone: (860) 685-2422;
Fax: (860) 685-2141;
E-mail: imukerji@wesleyan.edu

Our studies have initially focused on those functional groups, which have proven to be important in the study of nucleic acid structure. In particular, resonance Raman studies of quadruplex DNA (3-5) and A-tract DNA (6) have demonstrated the relative importance of the frequency shifts and intensity changes of the exocyclic amino and carbonyl functional groups. We have investigated the three purine bases, adenosine, guanosine and inosine, as a function of pH to study the effect of ring protonation and deprotonation on the frequencies and intensities of these functional groups. By examining these three bases, the effect of having one or both functional groups present can be probed separately (Figure 1). These studies reveal that the protonated states are characterized by distinct vibrational modes and under conditions of low and high pH values unusual tautomeric forms are stabilized, which are identified in the UVRR spectra.

We demonstrate the relevancy of such studies by examining a DNA duplex containing an A3T3 tract. DNA sequences containing A_n tracts have been shown to exhibit physical properties that are different from regular B-form DNA. The most striking observation is that such sequences exhibit reduced gel mobility, which has been attributed to a bending or curving of the DNA (12,13). Other physical properties, as identified by X-ray crystallography, include a narrowed minor groove, propeller twisting of the dA bases and formation of 3-centered H-bonds between the dA and dT base pairs (14-17). The A3T3 dodecamer is compared with a control dodecamer molecule that contains an alternating ATATAT sequence (AT)3 (18) in order to identify those UVRR spectral features that are unique to the A_n tract. We observe that the A3T3 dodecamer does have spectral features that are not detected in the (AT)3 dodecamer and interestingly, many of these modes are also detected in the protonated spectra of the purine bases. Because of these similarities and the resonance enhancement effect, the spectral features unique to the A3T3 dodecamer are assigned to the adenine residues in the A-tract.

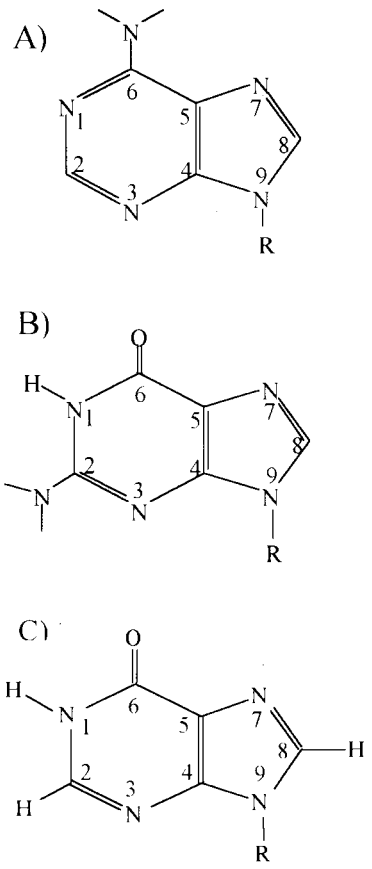

Figure 1: Structure of the three purine bases investigated in this study, A) adenosine, B) guanosine and C) inosine. For adenosine and guanosine the R group represents a 2′-deoxyribose, while for inosine the R group is ribose. In all cases the 5′-monophosphate derivative was studied.

Materials and Methods

Nucleotides and Polynucleotides

2′-Deoxyadenosine-5′-monophosphate (dAMP), 2′-deoxyguanosine-5′-monophosphate (dGMP) and inosine-5'-monophosphate-free acid (IMP) (Sigma) were used without further purification. For the low pH studies (≤ 7.0), a 1 mM solution of the 5′-nucleotide was prepared in 20 mM sodium cacodylate with 0.3 M Na_2SO_4 as an internal intensity and frequency standard. The pH was adjusted with HCl. For the high pH studies (> 7.0) a 1 mM solution of the 5′-nucleotide was prepared in 20 mM sodium borate with 0.3 M Na_2SO_4 as an internal intensity and frequency standard. The pH was adjusted with NaOH. At extreme low and high pH values, UVRR spectra were obtained immediately after preparation.

A3T3 and (AT)3 Dodecamers

The DNA dodecamers 5′-CGCAAATTTGCG-3′ (A3T3) and 5′-CGCATATATGCG-3′ ((AT)3) were synthesized in 1 μmol quantities by Integrated DNA Technologies. Tritylated oligomers were purified by HPLC using a PRP-1 semi-preparative column and a solvent system of 0.10 M ammonium acetate, pH 6.8 and acetonitrile. A continuous gradient from 100% ammonium acetate to 50% ammounium acetate/50% acetonitrile was used to elute the oligonucleotides from the column. The peak associated with the oligomer containing the trityl group was collected and the solvent was evaporated. The trityl group was removed by dissolving the oligomer in 80% acetic acid for 30 minutes, followed by solvent evaporation. After repeated washings with purified water and solvent evaporation, samples were dialyzed extensively against the desired buffer in a Spectrapor microdialyzer. Oligomers were at least 98% pure as shown by analytical gel chromatography. The oligonucleotide concentration of the UVRR samples was approximately 1.25×10^{-4} M and the samples were contained in a 10 mM cacodylate, pH 7.0, 0.3 M Na_2SO_4 buffer. Thermal denaturation monitored by UV-Vis absorption spectroscopy and analytical gel electrophoresis were performed before and after spectroscopy to characterize samples and no evidence of degradation was observed.

UV Resonance Raman Spectroscopy

A Nd:YLF pumped Ti:Sapphire laser system (Quantronix) was used to generate all the excitation wavelengths. For the 240-280 nm range the process of sum frequency generation using two Barium-borate (BBO) crystals was employed to triple the funda-

mental laser frequency. For the 207-230 nm range the fourth harmonic was generated by frequency doubling the second harmonic; both harmonics were generated with BBO crystals. The laser was operated at a repetition rate of 1 kHz at an average power of 1 mW. Spectra were recorded using a 1.25 m monochromator (SPEX 1250M, Instruments, SA) equipped with a 2400 grooves/mm grating. A 10 cm^{-1} spectral slit width (170 μm) was used. Data were recorded with a SPEX spectrum-1 liquid nitrogen cooled CCD detection system with a UV-enhanced 1024 × 256 pixel chip. Data were calibrated with acetone, ethanol and pentane and absolute frequencies are accurate to ±1 cm^{-1}. Relative frequency shifts are accurate to ± 0.25 cm^{-1}. Samples were contained in a stirred quartz cuvette (1 cm x 1cm) and were maintained at room temperature. Spectra shown result from 15-30 minutes of data collection. Data were acquired in a series of 2 or 3 cycles of 10 to 15 minutes each, if any changes in the spectra were observed between cycles, those spectra were discarded.

UVRR spectra of the A3T3 and (AT)3 dodecamers were obtained at 5°C through the use of an aluminum block cell holder and temperature was maintained with a circulating bath. Samples were contained in a cylindrical quartz microcuvette (NSG Precision Cells), which had a diameter of 0.3 cm. Samples were stirred continuously during spectral acquisition. Spectra shown result from 0.5 hours of data collection; the A3T3 spectrum is an average of three 0.5 hour spectra. Because the sample concentrations were not exactly the same, the difference spectrum between A3T3 and (AT)3 was generated using the phosphate band at 1031 cm^{-1}. Since the oligonucleotides are the same length, it was assumed that this band, which arises from backbone vibrations, would have the same intensity for both dodecamers.

Data manipulation and analysis were done using the program Grams/32 (Galactic Industries, NH). Spectra were normalized to unity using the SO_4^{2-} band, which is not affected by pH. Analysis of peak height intensities and frequency shifts were performed using the program Origin 6.0 (Microcal). Non-linear curve fit analyses were performed using the following equation, in which it was assumed that the vibrational frequency or mode intensity is related to the concentration of protonated (prot) and neutral nucleotide:

$$\nu_{obs} = \frac{\nu_{neutral} Ka + \nu_{prot}\left[H^+\right]}{Ka + \left[H^+\right]} \quad \text{or} \quad I_{obs} = \frac{I_{neutral} Ka + I_{prot}\left[H^+\right]}{Ka + \left[H^+\right]}$$

where $\nu_{neutral}$ ($I_{neutral}$) or ν_{prot} (I_{prot}) were taken as limiting constant values and were included as parameters in the fit. A similar set of equations was written for the conversion from the neutral to deprotonated form. The quality of the fit was judged by visual inspection and the χ^2 value.

Results and Discussion

dAMP

dAMP was investigated from pH 1 through 11 and over this pH range it is expected that the N1 position of dAMP will become protonated with a pK of ~4.0. At pH values less than 2.0, dAMP is expected to be doubly protonated at positions N1 and N7 (Figure 1) (19).

260 nm excitation. The largest changes in the 260 nm-excited spectra are observed from pH 1 through 5 (Figure 2), as expected from the associated protonation patterns. One of the most dramatic changes involves the 1603 cm^{-1} mode (pH 7.0), which exhibits a frequency shift and increases in intensity with decreasing pH. The assignment of this band as an -NH2 scissoring motion coupled with C5 = C6 ring stretching vibrations, is based upon the large frequency shift observed in D_2O (7). In these studies this $-NH_2$ mode shifts to higher frequency, 1614 cm^{-1}, and increases dramatically in intensity at pH values ≤ 4.0. In earlier studies similar shifts to higher frequency were observed and attributed to stronger H-bonding of the amino group (3,20,21,).

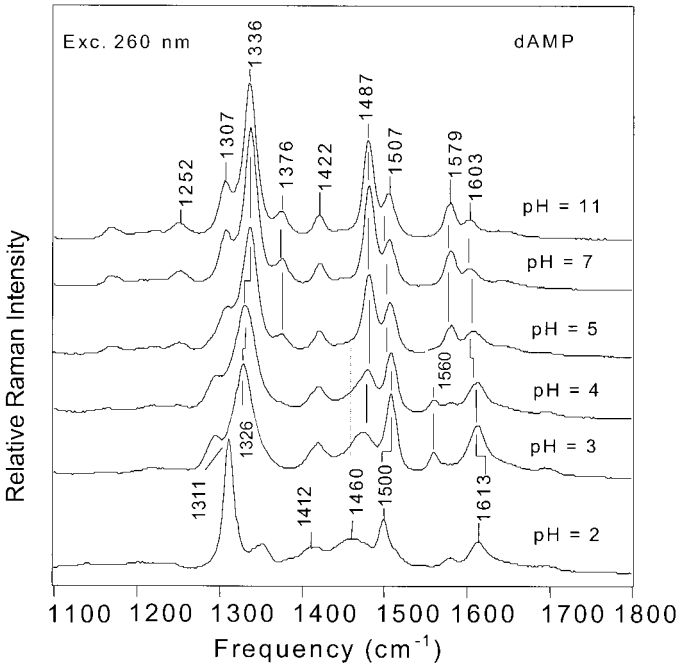

Figure 2: 260 nm-excited spectra of dAMP at pH values of 2, 3, 4, 5, 7 and 11. All spectra were normalized to the band at 981 cm^{-1} (not shown) of the sodium sulfate internal intensity standard. All spectra are plotted on the same scale. The concentration of dAMP was 1 mM. Buffer conditions as described in the text.

Protonation of dAMP also leads to distinct changes in the modes associated with ring stretching vibrations, which are strongly enhanced with 260 nm excitation. For example, the mode occurring at 1487 cm^{-1} (pH 7.0) is composed of N7 stretching motions and decreases in intensity at lower pH. This decrease in intensity is accompanied by the appearance of a band at 1460 cm^{-1}, leading to a broadening and apparent shift of the 1487 cm^{-1} band (Figure 2). These changes are detectable in the pH 4.0 spectra and are associated with N1 protonation; it is suggested that N1 protonation affects a mode primarily composed of N7 stretching motions because of the conjugated nature of the ring.

For all bases, protonation of the ring nitrogen leads to a localization of the π electrons in the double bonds, strengthening the

force constants which results in an increase in vibrational frequencies (10,22). Interestingly, the mode at 1580 cm^{-1} (pH 7.0) corresponding to C5 = C4 and C4-N3 stretching motions does not shift appreciably with N1 protonation (Figure 2); however a new band is observed at 1560 cm^{-1}. This band is only apparent at pH values of 5.0, 4.0 and 3.0 and is no longer observable at extremely low pH values (≤ 2.0), where it is expected that dAMP would be protonated at both the N1 and N7 positions.

Large spectral changes are also observed in the 1300 - 1400 cm^{-1} region. In this frequency range much of the stretching motions are associated with the imidazole ring. The spectral changes observed at the extremely low pH values (≤ 2.0) are distinct relative to those observed in the pH 3-5 range, consistent with a singly and doubly protonated state. The intensity ratio of the 1309 and 1338 cm^{-1} modes changes with protonation, such that 1309 cm^{-1} dominates at pH values ≤ 2.0 while the 1338 cm^{-1} dominates at neutral pH. The 1338 cm^{-1} mode is comprised of N7 - C5 and N7 = C8 stretching motions (7) and therefore the loss of intensity is probably associated with N7 protonation. At pH 3.0 the 1338 cm^{-1} mode is still intense and has frequency downshifted 10 cm^{-1}. The dependence of these frequency and intensity changes on pH yields a pK (4.0 ± 0.3) (Figure 3) that is consistent with previously determined values for N1 protonation (19). These observed protonation changes are also in agreement with previously reported spectral changes observed by Raman spectroscopy (10). These 260 nm-excited pH dependent spectra reveal three bands, which can be used for identifying the protonation state of adenine. The 1560 cm^{-1} mode is only observed with N1 protonation, while the 1309 cm^{-1} mode increases dramatically in intensity with N1 and N7 protonation. In addition, N1 protonation leads to the observation of a mode at 1460 cm^{-1}, which is most pronounced at pH values ≤ 2.0 although also observable at pH values where only the N1 position is expected to be protonated.

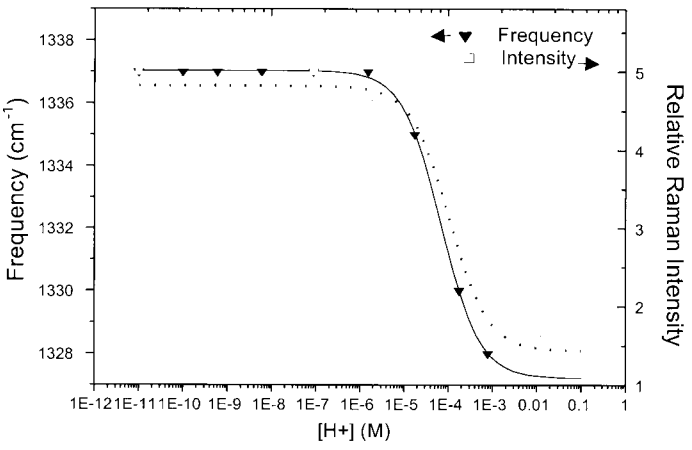

Figure 3: The intensity (□) and frequency (▼) of the 1338 cm^{-1} mode (pH 7.0) of dAMP as a function of H^+ concentration. Spectra were obtained using 260 nm excitation. The curves were analyzed as described in the text, yielding a pK value of 4.6 for the intensity curve and 3.7 for the frequency curve. These values are in good agreement with the expected values for N1 protonation of dAMP.

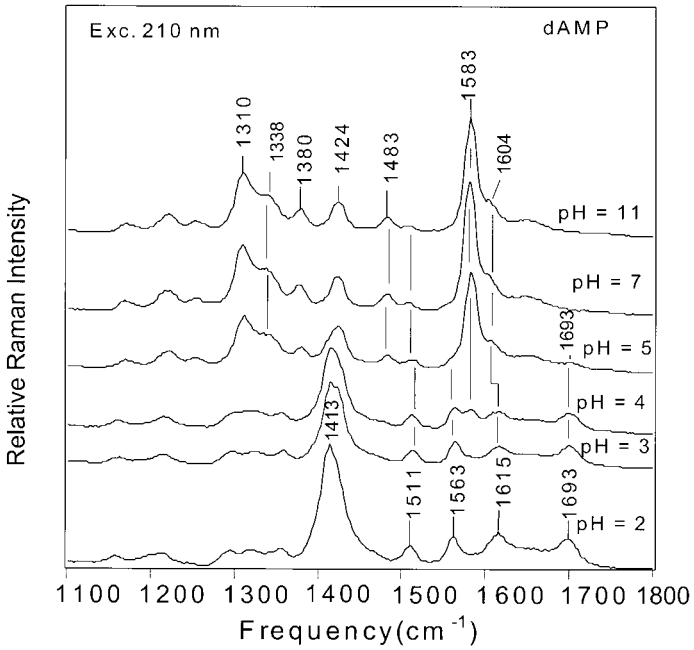

Figure 4: 210 nm-excited spectra of dAMP at pH values of 2, 3, 4, 5, 7 and 11. All spectra were normalized to the band at 981 cm^{-1} (not shown) of the sodium sulfate internal intensity standard. All spectra are plotted on the same scale. The concentration of dAMP was 1 mM. Buffer conditions as described in the text.

210 nm excitation. The most striking observation in the 210 nm-excited pH dependent spectra is the appearance of a band at 1693 cm^{-1} (Figure 4). The band is first observable in the pH 5.0 spectra and increases in intensity as the pH is lowered. This band has not been previously observed for adenosine and we tentatively assign this mode to the C6 = N stretch of the imino tautomeric form. The relatively high frequency of this mode is consistent with its assignment to a C = N stretching frequency (2). This assignment is further supported by the observed enhancement of the 1693 cm^{-1} mode at shorter wavelengths. The band, also detectable with 260 nm excitation, is considerably more enhanced with 210 nm excitation because of the alignment of the transition dipole. At shorter wavelengths the resonant electronic transition is polarized along the C6-NH_2 bond and would be expected to enhance vibrational motions along that axis (7). Similar imino stretching frequencies for the tautomeric forms of protonated cytidine have been previously observed using UVRR spectroscopy (2). We note that the increased frequency of the amino group, detected at 260 nm, is also consistent with formation of the imino tautomer. The detection of this form, associated with a unique Raman band at pH 5.0 and below, may have important implications for the formation of DNA triplexes containing CG*A^+ base triads. A detailed description of this mode awaits normal coordinate analysis of the protonated form of adenine.

dGMP

dGMP was investigated from pH 0.5 through pH 12 using excitation wavelengths of 260 and 210 nm. Over this pH range, it is expected that dGMP will become protonated at the N7 position at pH values ≤ 2.0, and deprotonated at the N1 position at pH values ≥ 10 (19).

260 nm excitation. With protonation of the N7 position the UVRR spectrum of dGMP is dramatically altered with the appearance of many new bands (Figure 5). The current discussion will focus on those bands for which the assignments are well-described. Many of the changes observed are similar to those observed for protonation of dAMP, as expected from the relatively similar electronic structure of the two purine residues. Of particular interest is the $-NH_2$ scissors mode, which was observed to increase in frequency with ring nitrogen protonation in the case of dAMP. Although the position on the ring is different (Figure 1), this mode also exhibits a frequency increase for dGMP. At pH 7.0 it occurs at 1602 cm^{-1}, while at pH 0.8 the mode has increased strongly in intensity and shifted to 1613 cm^{-1}. Therefore, similar to dAMP, this mode increases in frequency and intensity with stronger H-bonding and ring protonation.

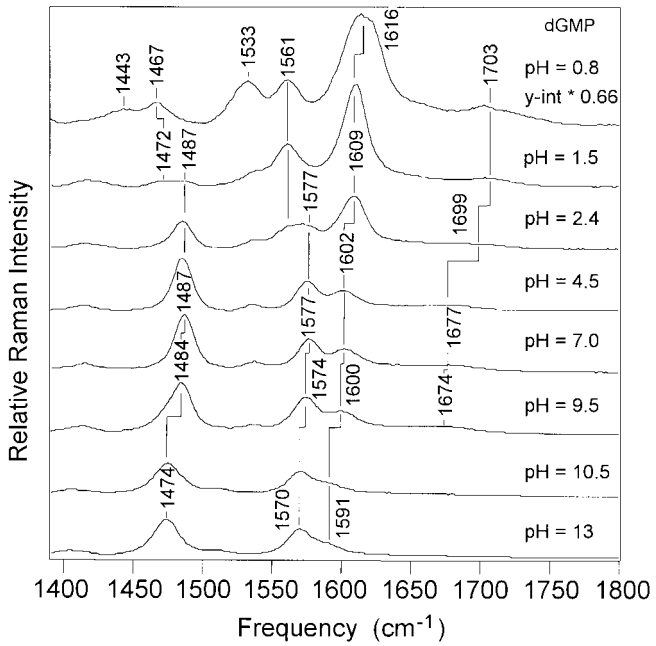

Figure 5: 260 nm-excited spectra of dGMP at pH values of 0.8, 1.5, 2.4, 4.5, 7.0, 9.5, 10.5 and 13. All spectra were normalized to the band at 981 cm^{-1} (not shown) of the sodium sulfate internal intensity standard. All spectra are plotted on the same scale; the spectrum obtained at a pH value of 0.8 has been multiplied by a y-scale factor of 0.66. The concentration of dGMP was 1 mM. Buffer conditions as described in the text.

Other changes at low pH are similar to those observed with dAMP and include a loss of intensity for the mode occurring at 1577 cm^{-1} (pH 7.0) and at 1487 cm^{-1} (pH 7.0). The 1577 cm^{-1} mode is centered on the central triene bond C2 = N3 - C4 = C5 - N7 = C8 and is strongly affected by protonation at the N7 position. Similar to dAMP, the loss of intensity at 1577 cm^{-1} is accompanied by the appearance of a mode at 1561 cm^{-1}. This 1561 cm^{-1} mode appears to be associated with the singly protonated state of both purines. The 1487 cm^{-1} mode, similar to the 1577 cm^{-1} modes, is comprised of N7 stretching motions. It has been shown to be sensitive to H-bonding at the N7 position (3) and normal coordinate analysis reveals it to have considerable imidazole ring character (7). As the pH is decreased, a band at 1467 cm^{-1} grows in, which we associate with the N7 protonated state. The decrease in intensity at 1487 cm^{-1} relative to the intensity increase at 1467 cm^{-1} as a function of pH yields a pK of 2.5, which is consistent with the expected pK value for N7 protonation for dGMP. A mode of similar frequency was associated with the protonated state of dAMP (Figure 2).

At high pH, the vibrational bands above 1450 cm^{-1} decrease in intensity (~ 30 %) and shift to lower frequency (Figure 5). The 1487 cm^{-1} (at pH 7.0) shifts to 1474 cm^{-1} and the triene mode observed at 1577 cm^{-1} shifts to 1570 cm^{-1}. These shifts plotted as a function of pH yield a pK value of 10.0, which is the value expected for N1-H deprotonation (Figure 6). N1-H deprotonation leads to a delocalization of the π electrons, which reduces the double bond nature of the ring and consequently, lowers the force constant and the vibrational frequency (10,22). Although these modes do not explicitly contain an N1 stretching coordinate the sensitivity to the deprotonation event results from the overall changes to the electronic configuration of the ring. Similarly, the $-NH_2$ scissoring vibration observed at 1603 cm^{-1} is also sensitive to ring deprotonation and shifts -10 cm^{-1}, becoming a shoulder on the main peak at 1570 cm^{-1}.

210 nm excitation. Higher energy electronic transitions of dGMP are polarized along the C = O bond leading to an enhancement of the mode occurring at 1681 cm^{-1} (pH 7.0), which is associated with localized C6 = O stretching motions (7). Thus, this excitation wavelength is preferred for monitoring the behavior of the C = O bond as a function of pH (Figure 7). Protonation of the N7 position results in a frequency increase of this mode, which shifts up to 1706 cm^{-1} at pH values ≤ 2.0. This behavior is consistent with ring protonation increasing the force constants of the bonds as a consequence of increased π electron localization on the ring (10,22).

At higher pH values the C = O mode experiences a dramatic decrease in intensity, such that it is no longer a distinct band at pH 11.0. It is expected that this mode would decrease in frequency, because of the increased delocalization of the π electrons leading to a reduction in the C = O force constant. A slight

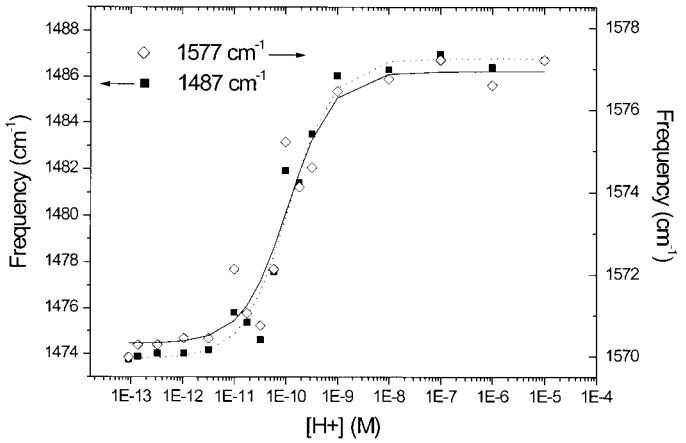

Figure 6: Frequency of 1577 (■) and 1487 cm^{-1} (◊) (pH 7.0) of dGMP plotted as a function of H^+ concentration. Spectra were obtained using 260 nm excitation. The curves were analyzed as described in the text, yielding a pK value of 10.0 ± 0.1 for the 1487 cm^{-1} mode and 10.0 ± 0.1 for the 1577 cm^{-1} mode. These values are in good agreement with the expected values for N1-H deprotonation of dGMP.

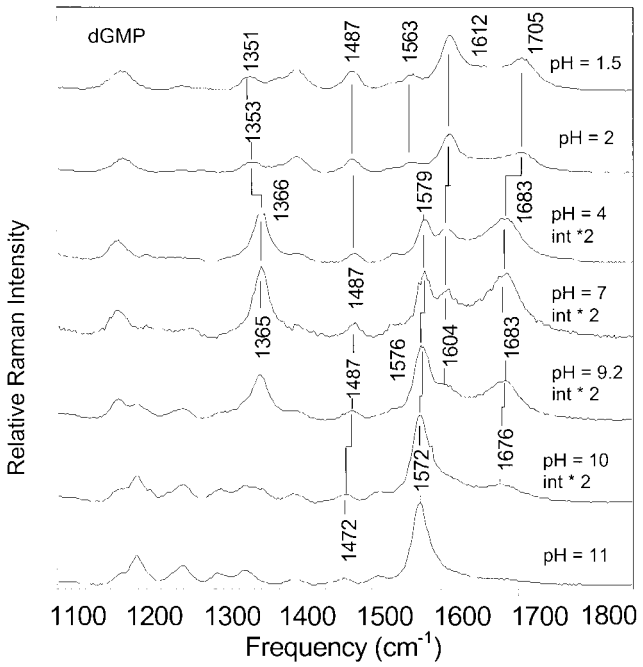

Figure 7: 210 nm-excited spectra of dGMP at pH values of 1.5, 2.0, 4.0, 7.0, 9.2, 10.0 and 11. All spectra were normalized to the band at 981 cm^{-1} (not shown) of the sodium sulfate internal intensity standard. All spectra are plotted on the same scale; the spectra obtained at pH values of 4.0, 7.0, 9.2, and 10.0 have been multiplied by a y-scale factor of 2.0. The concentration of dGMP was 1 mM. Buffer conditions as described in the text.

decrease in frequency (2 cm^{-1}) does occur; however the primary effect appears to be a substantial decrease in intensity (Figure 7). We suggest that this decrease in intensity does not result from a significant reduction in the enhancement of this mode, as this mode is not significantly enhanced with 260 nm excitation yet, the same behavior is observed. In addition, the enhancement of other modes observed with 210 nm excitation appears to be relatively unchanged at high pH. We attribute the dramatic intensity decrease of the C6 = O mode at pH values ≥ 10 to an increased population of the enolate tautomeric form. A detailed normal coordinate treatment of deprotonated dGMP in different tautomeric forms is in progress to confirm this assignment.

IMP

IMP was examined at 250 and 210 nm, as these wavelengths were previously determined to be optimal for enhancing in-plane base vibrations and the carbonyl-stretching mode, respectively (5). Protonation of the N7 position is expected to occur at pH 1.2 and deprotonation of N1 is expected to occur at pH 8.9. IMP provides an important counterpoint to dAMP and dGMP, as it does not have the exocyclic -NH_2 group but does have the exocyclic C = O (Figure 1).

250 nm excitation. IMP was monitored to confirm the behavior of the -NH_2 scissors mode as a function of pH. In the IMP 250 nm-excited UVRR spectrum a band at 1603 cm^{-1} is not observed (Figure 8), confirming that this mode in dGMP and dAMP arises from -NH_2 scissoring vibrations coupled with C = C bond stretching motions. The absence of the band further demonstrates that the observed frequency upshift of the -NH_2 mode in the other purines results from ring protonation and increased solvent effects.

210 nm excitation. The C6 = O mode is strongly enhanced at this wavelength and exhibits the largest change with pH. Protonation of the N7 position results in a significant broadening of the C6 = O band (Figure 8). Curvefitting of the C6 = O band (not shown) reveals the presence of a band at 1686 cm^{-1}, which shifts up to 1698 cm^{-1} upon protonation. This behavior is similar to that observed with N7 protonation of dGMP and corresponds to the increased localization of π electrons with protonation, leading to an increase in strength of the C = O force constant. The increased broadening of this mode is attributed to the appearance of an additional mode upon protonation (1614 cm^{-1}), which is similar to the 1560 cm^{-1} modes observed upon protonation of dGMP and dAMP. This mode occurs at higher frequency for IMP (1614 vs. 1560 cm^{-1}), because of the absence of the exocyclic amino group, which increases the frequency of the N7 imidazole ring stretching modes (23). At high pH values the IMP C6 = O band loses intensity; we attribute the loss of intensity to the formation of a detectable population of the enolate tautomer upon deprotonation, similar to dGMP.

Relationship to A-tract DNA

Using 260 nm excitation, we have studied two molecules $d[CGCAAATTTGCG]_2$ and $d[CGCATATATGCG]_2$, referred to as A3T3 and (AT)3, respectively. At this excitation wavelength the dA and dT residues are the dominant contributors to the UVRR spectrum. In previous x-ray crystallographic studies, the A3T3 duplex exhibited structural features characteristic of an A-tract DNA molecule, including a narrowed minor groove, pro-

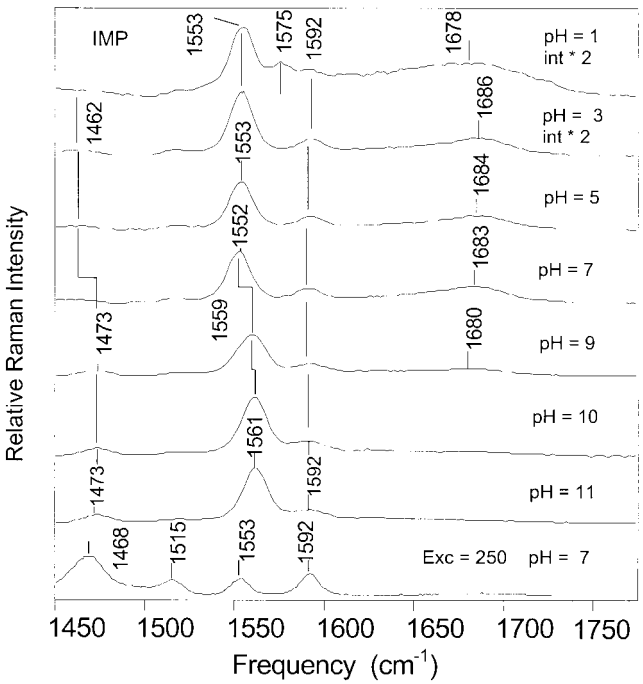

Figure 8: 210 nm-excited spectra of IMP at pH values of 1.0, 3.0, 5.0, 7.0, 9.0, 10.0 and 11. The bottom spectrum is IMP excited at 250 nm at a pH value of 7.0. All spectra were normalized to the band at 981 cm^{-1} (not shown) of the sodium sulfate internal intensity standard. All spectra are plotted on the same scale; the 210 nm-excited spectra obtained at pH values of 1.0 and 2.0 have been multiplied by a y-scale factor of 2.0. The concentration of IMP was 1 mM. Buffer conditions as described in the text.

peller twisting of the central A_5 residue and 3-centered hydrogen bonds between AT base pairs in the A_n tracts (15-17). The A3T3 and (AT)3 dodecamers were both studied at 5°C; at that temperature it has been previously shown that DNA molecules containing A_n-tracts are stabilized in a conformation that differs from regular B-form DNA. This conformation exhibits altered physical properties including anomalous gel migration (13) and a premelting thermal transition, which has been associated with the temperature-induced straightening of bent or curved DNA (24,25). In the current studies the (AT)3 molecule represents a control for the bent duplex, as it has the same base composition as the A3T3 duplex, but lacks sequential A residues. In addition, the alternating central AT sequence prevents the formation of 3-centered H-bonds.

Although the UVRR spectra of the two duplexes appear to be quite similar, there are subtle differences, which may illustrate the structural differences of the A-tract molecule (Figure 9). The most pronounced changes are observed in the region above 1550 cm^{-1}, in which the A3T3 molecule exhibits a frequency upshift of the exocyclic -NH_2 scissors vibration relative to the (AT)3 duplex, 1607 vs. 1604 cm^{-1}. The difference spectrum (Figure 9C) further confirms this +3 cm^{-1} frequency shift of the 'bent' A3T3 relative to the 'straight' (AT)3 molecule, by the presence of a peak at 1614 cm^{-1}. From the X-ray crystal structure, the environments of the three dA residues in the A3T3 are not homogeneous and the A5 residue exhibits the greatest amount of propeller twisting and potential for forming 3-centered H-bonds. This finding is further confirmed by NMR studies of amino group rotation which measured a higher activation enthalpy and entropy for the A5 residue (26). The dA residues in the (AT)3 sequences are expected to be in a B-form environment (18), therefore, subtraction of the (AT)3 spectrum removes the B-form contribution to the A3T3 spectrum and reveals those features that are unique to the A-tract. In particular, the frequency upshift of the -NH_2 scissors mode is associated with the A3T3 molecule and because of the resonance enhancement effect specifically associated with adenine residues and the A-tract. Similar upshifts in frequency of the -NH_2 scissors mode were observed in the low pH spectra of dAMP and dGMP and previously, such increases in frequency were associated with increased strength of H-bonding (20,21).

Interestingly, other spectral features observed in the spectra of dAMP at low pH are also detected in the A3T3 - (AT)3 difference spectrum (Figure 9C). These features include peaks at 1466 and 1347 cm^{-1} as well as increased intensity at 1310 cm^{-1}; all of these features were observed at pH values ≤ 3.0. From normal coordinate analyses, these modes are predicted to have considerable imidazole ring character, including N7 = C8 stretching motions (7). The 1309 cm^{-1} mode also contains N3 = C2 stretching motions. A more detailed description of these modes awaits a normal coordinate analysis of the protonated form. Although the relationship between the protonated state of dAMP and the A-tracts is not clear, increased solvent interactions with dAMP at low pH could potentially simulate some aspects of the environment of the A-tract. The difference spectrum further reveals

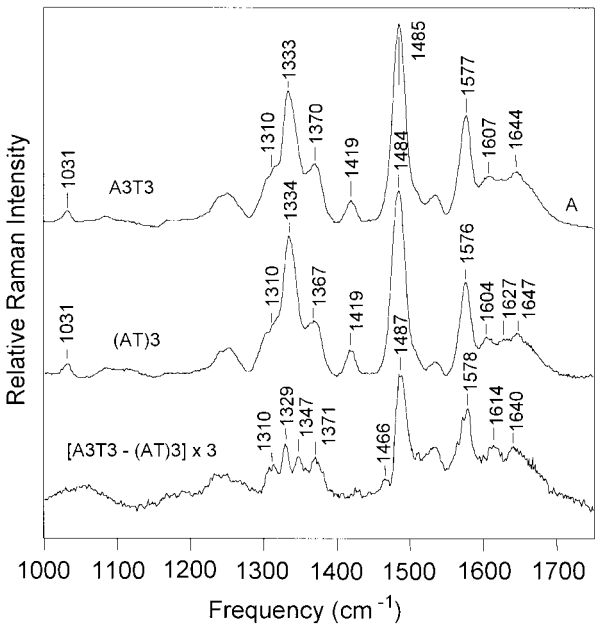

Figure 9: UVRR spectra of the (A) A3T3 (A-tract) and (B) (AT)3 (non A-tract) dodecamers measured with 260 nm excitation. Spectra are plotted on the same scale and have been normalized to the 981 cm^{-1} band of the sodium sulfate internal intensity standard (not shown). The difference spectrum (C) was generated using the phosphate band at 1031 cm^{-1}.

that the A3T3 spectrum is more intense than the (AT)3 spectrum relative to the phosphate mode at 1031 cm^{-1}. The greater intensity of the A3T3 spectrum is attributed to a reduced amount of base stacking and consequently, hypochromocity.

The frequency upshift of the dA-NH_2 mode identified in the A3T3 spectrum (Figure 9A) relative to the (AT)3 spectrum (Figure 9B) is suggestive of the potential formation of a 3-centered H-bond between the dA and dT residues in the A-tract. Further evidence for the presence of a 3-centered H-bond arises from the frequency of the thymine mode at 1644 cm^{-1} (Figure 9A). This mode arises from C = C and C4 = O stretching vibrations (7) and is downshifted in the presence of H-bonds (6,20). H-bonding leads to a decrease in the vibrational frequency because of the reduction in the C = O bond force constant. The frequency downshift (-3 cm^{-1}) of the dT C4 = O mode in the A3T3 dodecamer relative to the (AT)3 dodecamer is consistent with the putative formation of a 3-centered H-bond. The difference spectrum further reveals a peak at 1640 cm^{-1}, confirming the frequency downshift of the C4 = O mode observed in the A3T3 spectrum. In the non A-tract molecule a peak is also observed at 1627 cm^{-1}, which potentially arises from C = C stretching motions in the adenine ring (20). This mode is not observed in the A3T3 spectrum and leads to a trough in the difference spectrum at 1627 cm^{-1}. This mode appears to be associated with 'straight' DNA, as it is also observed in the 260 nm-excited UVRR spectrum of a DNA duplex dodecamer containing a 5′-T3A3-3′ tract (data not shown).

In summary, we have investigated the protonated, neutral and deprotonated states of 3 nucleic acid residues using UVRR spectroscopy. Through these investigations, vibrational bands, characteristic of the protonated state of dAMP and dGMP have been

identified. These bands can be used in future UVRR investigations of unusual DNA structures stabilized at low pH, such as DNA triple helices. Moreover, the stabilization of tautomeric forms at low and high pH is implicated in the UVRR spectra and these tautomeric forms also exhibit characteristic vibrational bands. Finally, we note that a DNA duplex containing an A3T3 tract exhibits many spectral features that were observed in the UVRR spectra of protonated dAMP. The comparison of a straight and bent DNA duplex has allowed us to identify vibrational bands that are potentially unique to these conformations. Normal coordinate analysis of the protonated state of adenine will improve the description and identification of these modes.

Acknowledgements

We are grateful to Dr. Alison Williams both for the purification of the A3T3 and (AT)3 dodecamers and for fruitful discussions.

References and Footnotes

1. Grygon, C.A., and Spiro, T.G., *Biopolymers 29*, 707-715 (1990).
2. Purello, R., Molina, M., Wang, Y., Smulevich, G., Fosella, J., Fresco, J.R., and Spiro, T.G., *J. Am. Chem. Soc. 115*, 760-767 (1993).
3. Mukerji, I., Shiber, M.C., Fresco, J.R., and Spiro, T.G., *Nucl. Acids Res. 24*, 5013-5020 (1996).
4. Wheeler, G.V., Jolles, B., and Chinsky, L., *J. Biomolec. Struct. Dyn. 14*, 91-99 (1996).
5. Mukerji, I., Sokolov, L., and Mihailescu, M.-R., *Biopolymers 46*, 475-487 (1998).
6. Chan, S.S., Austin, R.H., Mukerji, I., and Spiro, T.G., *Biophys. J. 72*, 1512-1520 (1997).
7. Fodor, S.P.A., Rava, R.P., Hays, T.R., and Spiro, T.G., *J. Am. Chem. Soc. 107*, 1520-1529 (1985).
8. Fodor, S.P.A., and Spiro, T.G., *J. Am. Chem. Soc. 108*, 3198-3205 (1986).
9. Suen, W., Spiro, T.G., Sowers, L.G., and Fresco, J.R., *Proc. Natl. Acad. Sci. USA 96*, 4500-4505 (1999).
10. Lord, R.C., and Thomas, G.J., Jr., *Spectrochim. Acta 23A*, 2552-2591 (1967).
11. Medeiros, G.C., and Thomas, G.J., Jr., *Biochim. Biophys. Acta 247*, 449-462 (1971).
12. Wu, H.-M., and Crothers, D.M., *Nature 308*, 509-513 (1984).
13. Hagerman, P.J., *Nature 321*, 449-450 (1986).
14. Nelson, H.C.M., Finch, J.T., Luisi, B.F., and Klug, A., *Nature 330*, 221-226 (1987).
15. Coll, M., Frederick, C.A., Wang, A.H.-J., and Rich, A., *Proc. Natl. Acad. Sci. USA 84*, 8385-8389 (1987).
16. Edwards, K.J., Brown, D.G., Spink, N., Skelly, J.V., and Neidle, S., *J. Mol. Biol. 226*, 1161-1173 (1992).
17. Tabernero, L., Verdaguer, N., Coll, M., Fita, I., van der Marel, G., van Boom, J. H., Rich, A., and Aymami, J., *Biochem. 32*, 8403-8410 (1993).
18. Yoon, C., Prive, G.G., Goodsell, D.S., and Dickerson, R.E., *Proc. Natl. Acad. Sci., USA 85*, 6332-6336 (1988).
19. Saenger, W. (1984) *Principles of Nucleic Acid Structure*. Springer Advanced Texts in Chemistry (Cantor, C. R., Ed.), Springer-Verlag, New York.
20. Toyama, A., Takeuchi, H., and Harada, I., *J. Mol. Struct. 242*, 87-98 (1991).
21. Mukerji, I., Shiber, M.C., Spiro, T.G., and Fresco, J.R., *Biochem. 34*, 14300-14303 (1995).
22. Shimanouchi, T., Tsuboi, M., and Kyogoku, Y., *Adv. Chem. Phys. VII*, 435-498 (1965).
23. Ulicny, J., Ghomi, M., Tomkova, A., Miskovsky, P., Turpin, P.Y., and Chinsky, L., *Eur. Biophys. J. 23*, 115-123 (1994).
24. Park, Y.-W., and Breslauer, K.J., *Proc. Natl. Acad. Sci. USA 88*, 1551-1555 (1991).
25. Chan, S.S., Breslauer, K.J., Austin, R.H., and Hogan, M.E., *Biochem. 29*, 6161-6171 (1993).
26. Michalczyk, R., and Russu, I.M. (1998) in *Structure, Motion, Interaction and Expression of Biological Macromolecules, Proceedings of the Tenth Conversation* (Sarma, R. H., and Sarma, M. H., eds), pp. 181-189, Adenine Press, Albany.